




# An Integrated Approach for Demand Response and Wind Curtailment Management in Distribution Systems

Osama. A. El-Kashty , Ahmed. A. Daoud , E. E. El-Araby 

Department of Electrical Engineering, Faculty of Engineering, Port Said University, Egypt

(osama.alkashty@eng.psu.edu.eg, a.daoud@eng.psu.edu.eg, [elsaid.elaraby@eng.psu.edu.eg](mailto:elsaid.elaraby@eng.psu.edu.eg))

Corresponding Author: E. E. El-Araby, Department of Electrical Engineering, Faculty of Engineering, Port Said University, Egypt

Tel: +20 1061460065,

[elsaid.elaraby@eng.psu.edu.eg](mailto:elsaid.elaraby@eng.psu.edu.eg)

Received: 06.05.2023 Accepted: 26.05.2023

**Abstract-** Studies have demonstrated that Demand Response (DR) can significantly influence the effectiveness and reliability of future intelligent distribution networks. Despite the increasing deployment of wind energy, the issue of curtailment continues to pose a challenge for utilities that have a high penetration of wind power. This study aims to propose an effective approach for utilizing DR to improve the operating status of distribution networks while simultaneously reducing curtailed wind energy. Thus, considering the curtailed wind energy, this paper proposes a wind curtailment reduction DRP (WCR-DRP) to modify the demand pattern in response to critical times when wind curtailment may occur due to generator ramp limits or minimum output power. In this study, to implement power system operation, an optimal power flow (OPF) problem is utilized while considering the availability of demand response (DR) programs, and the power flow and operational constraints related to the system are considered.

Formulating the optimization problem with two objective functions, including minimizing overall costs and reducing wind power curtailment, is achieved. The  $\epsilon$ -constraint method resolves this optimization problem. Finally, the suggested model is employed over the enhanced IEEE 33-bus test system to evaluate its efficacy. Four scenarios are conducted, examining various operational parameters to show the practicality of the suggested approach. Outcomes show that suggested model significantly enhances the operation of the electrical distribution system while establishing optimal employment of wind power.

**Keywords-** Demand Response (DR), price elasticity, optimal power flow (OPF), curtailed wind energy, multi-objective, distribution network.

## NOMENCLATURE

### Abbreviations

DRPs	Demand Response Programs
OPF	Optimal Power Flow
MOO	Multi-Objective Optimization
GAMS	General Algebraic Modelling System
MINLP	Mixed-Integer Non-Linear Programming
WCR	Wind Curtailment Reduction
RES	Renewable Energy Sources
PEM	Price Elasticity Model
VDI	Voltage Deviation Index
TOU	Time-of-Use
RTP	Real-Time Pricing
CPP	Critical Peak Pricing
NEOS	Network-Enabled Optimization System
IBDR	Incentive-Based Demand Response
PBDR	Price-Based Demand Response

### Indices and Sets

$t, T$	Index and set of time intervals
$tcr, Tcr$	Index and set of critical time at which wind curtailment may happen
$n, N$	Index and set of periods within the day
$i, j, I$	Indices and set of network buses
$S$	Slack buses set
$G$	Network generators sets
$W$	Set of buses connected wind energy
$Pp$	Peak period set
$Fp$	Flat period set
$Vp$	Valley period set

### Parameters, Variables, and Constants

$E$	Demand price elasticity
$E_{tt}$	Self-elasticity
$E_{t\hat{t}}$	Cross elasticity
$\rho_t^0, \rho_t$	Electricity charges before and after implementing DR at time $t$
$d_t^0, d_t$	Load before and after implementing DR at time $t$
$RU_g, RD_g$	Ramp-up and Ramp-down limits of generator $g$
$W_t$	Summation of generators output power at time $t$
$\alpha_{f, tcr}, \alpha_{v, tcr}$	Binary variables related to min output at flat and valley periods
$\beta_{p, tcr}, \beta_{f, tcr}, \beta_{v, tcr}$	Binary variables related to max ramp-up limits at peak, flat, and valley periods
$\gamma_{p, tcr}, \gamma_{f, tcr}, \gamma_{v, tcr}$	Binary variables related to max ramp-down limits at peak, flat, valley periods
$diff_{up(t)}$	Summation of ramp-up rates of all generators at time $t$
$diff_{dw(t)}$	Summation of ramp-down rates of all generators at time $t$
$Xp_t, Xf_t, Xv_t, Xp_{up_{tcr}}, Xp_{dw_{tcr}}$	Binary variables used to determine critical times at peak, flat, and valley periods.
$Cost_{Op}$	Total system operating cost (\$)
$Cost_{gen}$	Generation cost of generators (\$)
$Cost_{wc}$	Cost of system's wind curtailments (\$)
$Cost_{DR}$	Cost of implemented IBDRP (\$)
$TLR_t^{DR}$	Total load reduction due to IBDR program
$inc_p$	Customer incentives for reducing demand at peak period (\$/MWh)
$d_{i,t}^0$	Base load of bus $i$ at time $t$ before applying DR

$d_{i,t}$	Load of bus $i$ at time $t$ after applying DR (MW)
$\rho_n^0$	Electricity charge before applying DR (\$/MWh)
$\rho_p$	Electricity charge on the peak period (\$/MWh)
$\rho_f$	Electricity charge on the flat period (\$/MWh)
$\rho_v$	Electricity charge on the valley period (\$/MWh)
$\rho_{p,cr}$	Electricity charge at critical times of the peak period
$\rho_{f,cr}$	Electricity charge at critical times of the flat period
$\rho_{v,cr}$	Electricity charge at critical times of the valley period
$\rho_v^{lim}$	Electricity charge limit at valley period (\$/MWh)
$DR^{lim}$	Load reduction limit of DRP (MW)
$wvc$	Value of wind curtailment per MWh (\$/MWh)
$I_{ij,t}, S_{ij,t}$	Current and complex power distributed between buses $i$ and $j$ at time $t$
$P_{ij,t}, Q_{ij,t}$	Real and imaginary power distributed between buses $i$ and $j$ at time $t$
$P_{ij}^{Max}, Q_{ij}^{Max}, S_{ij}^{Max}$	Real, Imaginary, and Apparent power limits of line between bus $i$ and bus $j$
$V_{i,t}, \delta_{i,t}$	Voltage magnitude and phase angle of bus $i$ at time $t$ .
$Z_{ij}, \theta_{ij}$	Impedance magnitude and angle of the line from bus $i$ to bus $j$
$p_{g,t}, Q_{g,t}$	Real and imaginary power generation of generator $g$ at time $t$
$p_g^{min}, p_g^{max}$	Min and max active power generation limits of generator $g$
$Q_g^{min}, Q_g^{max}$	Min and max reactive power generation limits of generator $g$
$P_{i,t}^{wc}, P_{i,t}^w, P_{i,t}^{wcap}$	Wind power capacity, actual wind generated, and curtailed power of wind

## 1. Introduction

Implementation of renewable energy sources (RES) in power systems is becoming increasingly necessary in response to energy crisis and climate change [1]. Studies have found that global renewable capacity is predicted to increase by almost 2,400 GW between 2022 and 2027, demonstrating growing importance of RES in maintaining reliable and secure power systems [2]. Among the fastest-growing renewable sources, wind power has received significant attention from researchers studying its characteristics and requirements for integration into power grid [3]. Despite benefits of wind energy, a significant proportion of it is wasted due to technical security limitations and need for power system stability. Wind curtailment, in which power production from wind turbines is reduced below maximum amount that a system of properly operating wind turbines can produce, has become a major

challenge in integration of RES [4], it results in a significant reduction in economic and energy. In order to maintain system reliability, decreasing renewable energy production in any region of network is required to maintain equilibrium between supply and demand. Incorporation of more adaptable resources into system, including demand response and energy storage, can help address these issues [5,6].

Demand Response (DR) is a technique that opens up electricity market to consumer participation by decreasing peak loads or adjusting energy usage in response to dynamic pricing or other incentives [7]. DR can reduce customers' electric bill costs and decrease peak demand, eliminating the need to run expensive, high-emission-producing units, and avoiding or postponing the need for capital-intensive reinforcements. It also provides insurance against volatility of real-time market prices and helps mitigate risks associated

with unpredictable pricing for energy providers. [8]. DR can be employed as an ideal addition to erratic RES like wind. The need for further examination of various technical and financial advantages of DR in these systems is, therefore, necessary before its implementation. As systems with higher penetration of wind energy require close attention to ensure that DR manages difficult features of RES penetration, power grid corporations, and research institutions focus on how best to integrate these techniques [9-11]. There are two classes of DR: price-based (PB) and incentive-based (IB). PBDR programs use pricing signals such as RTP, TOU, and CPP to encourage customers to manage their electricity usage. In contrast, IBDR programs provide customers with monetary rewards or penalties for decreasing their electricity usage at peak times [12]. DR modeling is inspired by consumer behavior, elasticity is a useful method for understanding customer behavior. PBDR utilizes Price Elasticity Model (PEM) to evaluate how load responds to changes in price, while IBDR uses an expanded version of PEM that considers incentives and penalties [13].

### 1.1. Literature Review

In this literature, several studies that have investigated the use of price elasticity models in PBDR and IBDR programs are summarized. These studies have suggested various optimization models and evaluated performance of different pricing strategies and incentive mechanisms.

In [14], a DR program that merges PB and IB DR is proposed. It provides significant benefits for electricity providers that serve load and reduces location-based electricity price for customers while considering customer comfort. Authors in [15] propose a DR model with penalties and incentives and compare it with other DR models.

A mixed integer programming technique is utilized for solving DC optimal power flow problem to evaluate reliability. Model is tested on Iranian and IEEE RTS 24-bus test systems to prioritize DRPs. In [16], an economic framework for demand response program that considers demand elasticity with respect to price changes, incentives, and penalties is proposed. This model can be utilized to overcome difficulties in the operation of the market including, system reliability, security, and inadequate spinning reserves. In [17], a demand response approach integrated with an economic dispatch problem is presented, with wind energy and system reliability as key considerations. The IEEE 24-bus Reliability Test System is used as a simulation system to check model effectiveness. Authors in [18] propose an IBDR model using a PEM to analyze incentives' impact on customer demand sensitivity. The model differentiates economic and technical performance and suggests pricing strategies. The model is evaluated on IEEE 33 distribution system and assessed from customer and utility perspectives. Authors in [19] propose a real-time pricing model for demand response that optimizes pricing using elasticity and two types of DR. It can manage demand-side resources and facilitate renewable energy integration in smart grids. In [20], an optimal TOU approach is suggested to reduce power loss, variations in voltage, and difference between peak and valley values of

distribution systems. An IEEE 14-bus system is utilized to evaluate suggested model performance. In [21], economic effects of high wind power levels on distribution system are analyzed using a PB-DRP. An optimization problem is suggested to reduce system's operating costs, and simulation results show a decrease in operating cost and an enhancement to grid's ability to integrate more wind power. Authors in [22] introduce a stochastic model for DR scheduling in systems with significant wind power capacity. The model considers PB and IB DR programs, and simulation outcomes show reduced costs and emissions. It effectively optimizes resource scheduling. Authors in [23] propose a multi-timescale scheduling model that combines demand response and robust optimization to address wind power integration uncertainty. Simulations show cost reduction and improved integration. The model optimizes resource scheduling in high-wind power penetration systems.

### 1.2. Motivation and Contributions

The motivation for our proposed model stems from the need to improve the economic and technical performance of distribution systems integrated with wind energy. While some studies have proposed optimization models for wind energy integration, there is a lack of a demand response program (DRP) that encourages load modification during critical times to avoid wind curtailments. Such a DRP can ensure reliable and economic distribution system operation. Furthermore, both technical and economic aspects need to be considered for enhancing renewable energy integration.

This study proposes a Wind Curtailment Reduction Demand Response Program (WCR-DRP) to address wind energy curtailment challenges in high wind energy penetration utilities. At first, critical times at which wind curtailments may occur are determined, and then DR is applied based on identified critical times and the period during which they occur to avoid wind curtailments.

WCR-DRP is a modified TOU- PBDR technique that considers prices at normal and critical times (at which wind curtailments may happen). It classifies load curve into peak, valley, and flat durations using half-ladder membership function technique and utilizes an OPF problem to implement power system operation. A MINLP model is used to formulate multi-objective optimization problem with  $\epsilon$ -constraint method used to solve it, and a fuzzy satisfactory technique is utilized to choose best solution. The suggested approach is evaluated on enhanced IEEE 33-bus test system under various operational scenarios.

## 2. Methodology

This part contains methodology employed in this study, encompassing problem description and formulation of DR program.

### 2.1. Problem Description

Integrating wind power into electrical network is essential for achieving a sustainable energy future, but it poses

challenges due to its intermittent and variable nature. One of main challenges is wind curtailment. This can lead to a waste of clean energy and reduce power grid efficiency and reliability. Wind curtailments are correlated with certain situations related to minimum power limit and limits for power output ramp-up and ramp-down of generators, as explained below.

Consider a particular power system with wind power generation of 10 MW and a ramp-down/up limit of 30 MW.

Figure.1 illustrates a segment of the daily load profile (over a 5-hour period) from times t1 to t5 for this system. The y-axis represents the load (in MW) while the x-axis denotes time (in hours).

For instance, at times t3 and t4, the load is 70 MW and 30 MW respectively. Assuming the wind power to be 10 MW, the required generation from conventional sources would be 60 MW and 20 MW at t3 and t4 respectively. Here, the ramp-down power is 60 - 20 = 40 MW which exceeds the ramp-down limit of 30 MW. Therefore, to maintain the balance and stay within the ramp-down limit, the generation at t4 needs to be increased to 30 MW resulting in wind curtailment of 10 MW at t4 .

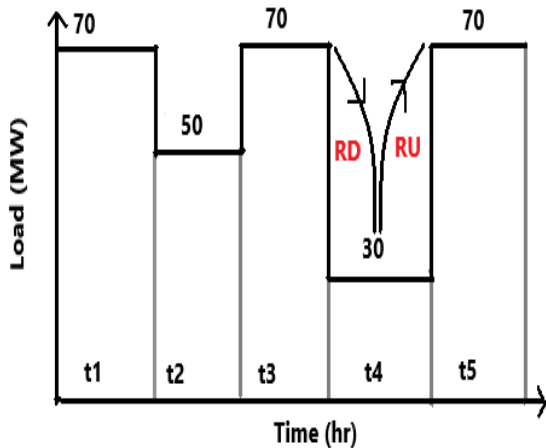


Fig. 1. Hourly load curve

Similarly, between t4 and t5, the required generation from conventional sources should be 20 MW and 60 MW respectively. The ramp-up power in this case is 60 - 20 = 40 MW which surpasses the ramp-up limit of 30 MW. Consequently, to preserve the balance and comply with the ramp-up limit, the generation at t4 must be raised to 30 MW leading to wind curtailment of 10 MW at t4.

Finally, considering only the minimum power output limit of generators to be 25 MW, while the wind power is 10 MW, the required conventional power at t4 would be 20 MW which falls below the minimum power limit (25 MW). Therefore, the generator power output must be increased to 25 MW resulting in wind curtailment of 5 MW at time t4.

This example demonstrates that wind power curtailment can occur due to certain situations, as below:

2.1.1 Ramp-Up Constraints

If summation of ramp-up rates of generators is greater than ramp-up limit as in Eq. (1),

$$\sum_g p_{g,t+1} - p_{g,t} > \sum_g RU_g, \forall g \in G, \forall t \in T \tag{1}$$

2.1.2 Ramp-Down Constraints

If summation of ramp-down rates of generators is greater than ramp-down limit as in Eq. (2),

$$\sum_g p_{g,t-1} - p_{g,t} > \sum_g RD_g, \forall g \in G, \forall t \in T \tag{2}$$

2.1.3. Min Power Constraint of Generators

If overall power output of all generators is less than minimum output power of generators as in Eq. (3),

$$\sum_g p_{g,t} < \sum_g p_g^{min}, \forall g \in G, \forall t \in T \tag{3}$$

where  $p_g^{min}$  is the lower power bound of the unit  $g$  (MW)

In these cases, one solution to balance load and ensure that output power is within limits for power output ramp-up and ramp-down of the generators is to increase output power of generator(s) at time  $t$  with capability to increase their output quickly while curtailing power output of wind generators to compensate for the excess power ( $P_t^{wc} > 0$ ).

This is because wind generators are often the most flexible and responsive generators in system, and can quickly adjust their output to compensate for fluctuations in power output of other generators.

To avoid curtailment, DR programs can be used to adjust load during critical times, the need to increase generation can be reduced, and wind power curtailment can be avoided.

2.2. Proposed DR Program

This section describes the proposed approach for reducing wind curtailment through a DR strategy, known as the Wind Curtailment Reduction DRP (WCR-DRP).

The proposed model suggests that DR can be used to address the technical constraints of generators, such as minimum load requirements or ramping limits.

This approach recognizes that high wind power periods do not necessarily correspond to periods of low demand and that demand response measures must be implemented carefully to make sure that they do not compromise reliability or stability of power grid. The use of OPF allows for a more precise determination of generator output and ramping limits, which can help reduce need for curtailment or increase output of other generators. The time at which generator output just equals ramp-down and ramp-up limits is identified. If this time falls within a valley or flat period of load curve, electricity prices at these times are adjusted to increase demand during these periods to reduce wind power curtailments. However, if the time falls within a peak period, there will be two different

scenarios. All cases of critical times associated with ramp limits will be discussed below.

The time at which the curtailment may occur is referred to as critical time (*tcr*). There are three cases associated with periods at which wind curtailments occur:

- Case 1: If *tcr* occurs at a peak period (*Pp*), there are two possible scenarios. The basic idea of reducing wind curtailment events is to increase power consumption during periods of high wind curtailment to make the best use of renewable power. However, increasing consumption during peak periods may lead to a new peak load, which could affect system security and reliability. Accordingly, a suggested technique is presented:

a) If *tcr* ∈ *Pp* is due to ramp-down constraints

If (*tcr* ∈ *Pp*), electricity prices are modified at time (*tcr* − 1) to motivate customers to move their load to different hours.

b) If *tcr* ∈ *Pp* is due to ramp-up constraints

If (*tcr* ∈ *Pp*), electricity prices are modified at time (*tcr* + 1) to motivate customers to move their load to different hours.

- Case 2: If *tcr* occurs during at the flat period *Fp*, electricity prices at this time are modified to motivate customers to increase their load consumption by shifting their load to this time.
- Case 3: If *tcr* occurs at valley period *Vp*, electricity prices at this time are modified to motivate customers to increase their load consumption by shifting their load to this time.

To build formulation of the proposed model, let's introduce the following variables and binary variables to represent critical times of minimum output and ramping constraints for generators.

2.2.1. Critical Time of Minimum Power of Generators

*W<sub>t</sub>*: This variable represents the summation of generator's output power at time *t*, as in Eq. (4).

$$W_t = \sum_g p_{g,t} \quad , \forall g \in G, \forall t \in T \quad (4)$$

It is more common for total generator output power to be close to, if not at, its maximum power output during peak periods to meet the high electricity demand.

Thus, we introduce two binary variables that indicate whether minimum power output of generators occurs during flat or valley periods. These binary variables can be defined as follows:

*α<sub>f,tcr</sub>*, and *α<sub>v,tcr</sub>*, these binary variables take on value 1 if summation of generators output power at time *t* equal to minimum generators output power for all generators at flat and valley times, respectively, as in Eq. (5) and Eq. (6).

$$\alpha_{f,tcr} = \left\{ \begin{array}{l} 1 \text{ if } W_t = \sum_g p_g^{min}, 0 \text{ otherwise} \end{array} \right\} \quad , \forall t, tcr \in Fp \quad (5)$$

$$\alpha_{v,tcr} = \left\{ \begin{array}{l} 1 \text{ if } W_t = \sum_g p_g^{min}, 0 \text{ otherwise} \end{array} \right\} \quad , \forall t, tcr \in Vp \quad (6)$$

2.2.2. Critical Time of Ramp-Up Constraints

*diff<sub>up</sub>(t)*: This variable represents difference in generator output power between two consecutive time intervals as given in Eq. (7), where *t* denotes current time interval. Specifically, it calculates sum of output power differences for all generators between time *t* and time *t* + 1.

*β<sub>p,tcr</sub>*, *β<sub>f,tcr</sub>* and *β<sub>v,tcr</sub>*: These binary variables take on value 1 if the difference in generator output power between time *t* and time *t* + 1 is equal to the sum of ramp-up limits (RU) for all generators at peak, flat, and valley times, respectively as introduced in Eq. 8 to Eq.10.

$$diff_{up}(t) = \sum_g p_{g,t+1} - p_{g,t} \quad , \forall g \in G, \forall t \in T \quad (7)$$

$$\beta_{p,tcr} = \left\{ \begin{array}{l} 1 \text{ if } diff_{up}(t) = \sum_g RU_g, 0 \text{ otherwise} \end{array} \right\} \quad , \forall t, tcr \in Pp \quad (8)$$

$$\beta_{f,tcr} = \left\{ \begin{array}{l} 1 \text{ if } diff_{up}(t) = \sum_g RU_g, 0 \text{ otherwise} \end{array} \right\} \quad , \forall t, tcr \in Fp \quad (9)$$

$$\beta_{v,tcr} = \left\{ \begin{array}{l} 1 \text{ if } diff_{up}(t) = \sum_g RU_g, 0 \text{ otherwise} \end{array} \right\} \quad , \forall t, tcr \in Vp \quad (10)$$

2.2.3. Critical Time of Ramp-Down Constraints

*diff<sub>dw</sub>(t)*: This variable represents difference in generator output power between two consecutive time periods, as in Eq. (11), where *t* denotes the current time period. Specifically, it calculates sum of the output power differences for all generators between time *t* − 1 and time *t*.

*γ<sub>p,tcr</sub>*, *γ<sub>f,tcr</sub>*, and *γ<sub>v,tcr</sub>*: These binary variables take on value 1 if the difference in generator output power between time *t* − 1 and time *t* is equal to summation of ramp-down limits (RD) for all generators at peak, flat, and valley times, respectively, as given in Eq. (12) to Eq. (14).

Therefore, we can formulate relationships between these variables and binary variables as follows :

$$diff_{dw(t)} = \sum_g p_{g,t-1} - p_{g,t} \quad , \forall g \in G, \forall t \in T \quad (11)$$

$$\gamma_{p, tcr} = \left\{ \begin{array}{l} 1 \text{ if } diff_{dw(t)} = \sum_g RD_g, 0 \text{ otherwise} \\ \end{array} \right\} \quad , \forall t, tcr \in Pp \quad (12)$$

$$\gamma_{f, tcr} = \left\{ \begin{array}{l} 1 \text{ if } diff_{dw(t)} = \sum_g RD_g, 0 \text{ otherwise} \\ \end{array} \right\} \quad , \forall t, tcr \in Fp \quad (13)$$

$$\gamma_{v, tcr} = \left\{ \begin{array}{l} 1 \text{ if } diff_{dw(t)} = \sum_g RD_g, 0 \text{ otherwise} \\ \end{array} \right\} \quad , \forall t, tcr \in Vp \quad (14)$$

Finally, before formulating the proposed DRP equation, some binary variables are set to handle the time at which WCR-DRP will occur which is given in Eq. (15) to Eq. (19)

$$Xf_t = \left\{ \begin{array}{l} 1 \text{ if } \alpha_{f, tcr} \text{ or } \beta_{f, tcr} \text{ or } \gamma_{f, tcr} = 1 \\ 0 \text{ otherwise} \end{array} \right\} \quad (15)$$

$$Xv_t = \left\{ \begin{array}{l} 1 \text{ if } \alpha_{v, tcr} \text{ or } \beta_{v, tcr} \text{ or } \gamma_{v, tcr} = 1 \\ 0 \text{ otherwise} \end{array} \right\} \quad (16)$$

$$Xp_{up_{tcr}} = \left\{ \begin{array}{l} 1 \text{ if } \beta_{p, tcr} = 1 \\ 0 \text{ otherwise} \end{array} \right\} \quad (17)$$

$$Xp_{dw_{tcr}} = \left\{ \begin{array}{l} 1 \text{ if } \gamma_{p, tcr} = 1 \\ 0 \text{ otherwise} \end{array} \right\} \quad (18)$$

$$Xp_t = Xp_{up_{tcr-1}} + Xp_{dw_{tcr+1}} \quad (19)$$

These constraints ensure that  $Xf_t$  is set to 1 during flat period when the restrictions on ramp-up and ramp-down rates, and minimum generated power are at their thresholds, and  $Xv_t$  is set to 1 during valley times when the restrictions on ramp-up and ramp-down rates, and minimum generated power are at their thresholds,  $Xp_{up_{tc}}$  is set to 1 only if the ramping-up constraint is met at peak times and  $Xp_{dw_{tc}}$  is set to 1 only if the ramping-down constraint is met at peak times. Thus, these binary variables are used to identify critical times during which demand change is needed to avoid wind curtailment.

In this study, load response model based on PEM is applied which is very common and effective in load modeling and is applied in various DRPs, in which overall load response model for PB/IB DRPs is in Eq. (20).

$$d_t = d_t^o \cdot \left( 1 + \sum_{t=1}^{24} Ett \cdot \frac{[\rho_t - \rho_t^o + inc_t]}{\rho_t^o} \right) \quad (20)$$

In case where a day is consists of three periods: peak period ( $Pp$ ), flat period ( $Fp$ ), and valley period ( $Vp$ ), elasticity coefficient matrix becomes:

$$E = \begin{bmatrix} Epp & Epf & Epv \\ Efp & Eff & Efv \\ Evp & Evf & Evv \end{bmatrix}$$

The proposed DRP equation involves introducing new electricity prices ,  $\rho_{n,cr}$ , during these critical times at each day period, in which  $\rho_{p,tcr}$ ,  $\rho_{f,tcr}$ , and  $\rho_{v,tcr}$  are electricity prices during critical time at peak, flat, and valley intervals, which can make customers change their demand during critical times when probability of wind curtailment is high. Thus, electricity price at each period could have two different values that depend on value of  $Xp_t$ ,  $Xf_t$ , and  $Xv_t$ , as presented in Eq. (21) to (24):

$$\rho_{n,t} = \rho_n * (1 - Xn_t) + \rho_{n,tcr} * Xn_t \quad , \forall n \in N \quad (21)$$

$$d_{i,p,t} = d_{i,n,t}^o \cdot \left\{ 1 + Epp \cdot \frac{[\rho_{p,t} - \rho_p^o]}{\rho_p^o} + Epf \cdot \frac{[\rho_{f,t} - \rho_f^o]}{\rho_f^o} + Epv \cdot \frac{[\rho_{v,t} - \rho_v^o]}{\rho_v^o} \right\} \quad , \forall i \in I, n \in N, \forall t \in T \quad (22)$$

$$d_{i,f,t} = d_{i,f,t}^o \cdot \left\{ 1 + Efp \cdot \frac{[\rho_{p,t} - \rho_p^o]}{\rho_p^o} + Eff \cdot \frac{[\rho_{f,t} - \rho_f^o]}{\rho_f^o} + Efv \cdot \frac{[\rho_{v,t} - \rho_v^o]}{\rho_v^o} \right\} \quad , \forall i \in I, n \in N, \forall t \in T \quad (23)$$

$$d_{i,v,t} = d_{i,v,t}^o \cdot \left\{ 1 + Evp \cdot \frac{[\rho_{p,t} - \rho_p^o]}{\rho_p^o} + Evf \cdot \frac{[\rho_{f,t} - \rho_f^o]}{\rho_f^o} + Evv \cdot \frac{[\rho_{v,t} - \rho_v^o]}{\rho_v^o} \right\} \quad , \forall i \in I, n \in N, \forall t \in T \quad (24)$$

The approach outlined above seeks to reduce wind curtailment events depending on load response to electricity price changes during periods of high wind curtailment probability. This model can reduce curtailments and make better use of renewable power.

### 2.3. Optimization Problem

Model is formulated as a multi-objective optimal power flow problem in which objectives are minimization total system operating cost and wind curtailed power. Different scenarios are studied to check suggested model effect.

#### 2.3.1. Objective Function

Minimization overall operating cost of the system and wind-curtailed power are the objective functions, as in Eq. (25) and Eq.(26)

$$\min OF \quad (25)$$

$$OF = \{OF_1 = Cost_{Op}, OF_2 = P_{wc}\} \quad (26)$$

Total operating cost is divided into three parts, as in Eq. (27).

$$Cost_{op} = (Cost_{gen} + Cost_{wc} + Cost_{DR}) \quad (27)$$

First part describes cost of generating electricity from thermal units (the cost of fuel), as in Eq. (28).

$$Cost_{gen} = \sum_{g,t} a_g(p_{g,t})^2 + b_g p_{g,t} + c_g \quad (\$)$$

$$\forall g \in G, \forall t \in T \quad (28)$$

Second part stands for wind curtailments costs of wind turbines, as in Eq. (29).

$$Cost_{wc} = \sum_{i,t} P_{i,t}^{wc} \cdot vwc \quad (\$) \quad \forall i \in W, \forall t \in T \quad (29)$$

Last part is the total DR cost if an IBDR scenario is considered, which is overall reduction in load during peak time (MWh) multiplied by incentive rate (\$/MWh), as in Eq. (30).

$$Cost_{inc} = \sum_t TLR_t^{DR} \cdot inc_t \quad (\$) \quad , \forall t \in T \quad (30)$$

Total load reduction in peak periods due to normal incentives is calculated, as in Eq. (31).

$$TLR_t^{DR} = \sum_i \left\{ -d_{i,t}^o \cdot Epp \cdot \frac{inc_p}{\rho_t^o} \right\} \quad \forall t \in Pp, \forall i \in I \quad (31)$$

Finally, total wind-curtailed power is the total wind power curtailed at each bus for the entire duration, as given in Eq. (32).

$$P_{wc} = \sum_{i,t} P_{i,t}^{wc} \quad \forall i \in W, \forall t \in T \quad (32)$$

### 2.3.2. Constraints

In this part, limitations and constraints that were taken into account in the optimization problem are discussed, as below:

#### 2.3.2.1. Power Flow Constraints

Active, reactive, and apparent power flow limits are considered, as in Eq. (33) to Eq. (36).

$$-P_{ij}^{Max} \leq P_{ij,t} \leq P_{ij}^{Max} \quad , \forall i, j \in I, \forall t \in T \quad (33)$$

$$-Q_{ij}^{Max} \leq Q_{ij,t} \leq Q_{ij}^{Max} \quad , \forall i, j \in I, \forall t \in T \quad (34)$$

$$-S_{ij}^{Max} \leq S_{ij,t} \leq S_{ij}^{Max} \quad , \forall i, j \in I, \forall t \in T \quad (35)$$

$$\text{Where } S_{ij,t} = \sqrt{(P_{ij,t}^2 + Q_{ij,t}^2)} \quad (36)$$

#### 2.3.2.2. Constraints on Ramping Up and Ramping Down

The maximum ramping up or ramping down limits define maximum rate at which generators can increase or decrease power, as in Eq. (37) and Eq. (38).

$$p_{g,t} - p_{g,t-1} \leq RU_g \quad , \forall g \in G, \forall t \in T \quad (37)$$

$$p_{g,t-1} - p_{g,t} \leq RD_g \quad , \forall g \in G, \forall t \in T \quad (38)$$

#### 2.3.2.3. Min/Max Power Constraints

Active and reactive generated power from thermal units must be within certain limits, as in Eq. (39) and Eq. (40).

$$p_g^{min} \leq p_{g,t} \leq p_g^{max} \quad , \forall g \in G, \forall t \in T \quad (39)$$

$$Q_g^{min} \leq Q_{g,t} \leq Q_g^{max} \quad , \forall g \in G, \forall t \in T \quad (40)$$

#### 2.3.2.4. Wind Energy Constraints

Wind power curtailment is the excess of available power from wind over actual power generated from wind turbines, as given in Eq. (41) to Eq. (43).

$$P_{i,t}^{wc} = P_{i,t}^{wcap} - P_{i,t}^w \quad , \forall i \in W, \forall t \in T \quad (41)$$

$$0 \leq P_{i,t}^w \leq P_{i,t}^{wcap} \quad , \forall i \in W, \forall t \in T \quad (42)$$

$$0 \leq P_{i,t}^{wc} \leq P_{i,t}^{wcap} \quad , \forall i \in W, \forall t \in T \quad (43)$$

#### 2.3.2.5. Voltage Constraints

Magnitude and angle of voltage at every bus at different times are limited by allowed voltage levels, as in Eq. (44) and Eq. (45), and voltage of the slack bus is maintained constant at  $1 \angle 0 p.u$  at different periods as in Eq. (46)

$$V_{min} \leq V_{i,t} \leq V_{max} \quad , \forall t \in T, \forall i \in I \quad (44)$$

$$\delta_{min} \leq \delta_{i,t} \leq \delta_{max} \quad , \forall t \in T, \forall i \in I \quad (45)$$

where  $V_{min}, \delta_{min}$  and  $V_{max}, \delta_{max}$  indicate minimum and maximum voltage thresholds that distribution system can sustain, respectively.

$$V_{i,t} = 1 \angle 0 p.u \quad , \forall i \in S \quad (46)$$

#### 2.3.2.6. Balance Constraints

Power balance at diverse system buses and time points are indicated as in Eq. (47) and Eq. (48).

$$P_{i,t}^g + P_{i,t}^w - d_{i,t} = \sum_j P_{ij,t} \quad \forall g \in G, \forall t \in T, i, j \in I \quad (47)$$

$$Q_{i,t}^g - Q_{i,t}^D = \sum_j Q_{ij,t} \quad , \forall g \in G, \forall t \in T, i, j \in I \quad (48)$$

Active and reactive power distribution on line is determined as in Eq. (49) and (50).

$$P_{ij,t} = \frac{V_{i,t}^2}{Z_{ij}} \cos(\theta_{ij}) - \frac{V_{i,t} * V_{j,t}}{Z_{ij}} \cos(\theta_{ij} + \angle \delta_{i,t} - \angle \delta_{j,t})$$

$$i, j \in I, \forall t \in T \quad (49)$$

$$Q_{ij,t} = \frac{V_{i,t}^2}{Z_{ij}} \sin(\theta_{ij}) - \frac{V_{i,t} * V_{j,t}}{Z_{ij}} \sin(\theta_{ij} + \angle\delta_{i,t} - \angle\delta_{j,t}) - \frac{b * V_{i,t}^2}{2} \quad \forall i, j \in I, \forall t \in T \quad (50)$$

2.3.2.7. DR Constraints

The first two constraints in Eq. (51) and Eq. (52) are related to incentive-based DR, where total load reduction (TLR) due to DR program should not exceed a predefined limit, and rate should be non-negative and less than or equal to another predefined limit.

The following constraints are related to price-based DR: Implementation of a TOU pricing scheme is intended to achieve load shifting in electricity grid. To ensure that this goal is met. Cost of electricity at peak times must be higher than cost at flat times, and cost at flat times must be higher than cost at valley times, this can be expressed mathematically as Eq. (53) and Eq. (54). To prevent that substantial price differences between peak and valley times cause a reversal of load between these periods, a constraint on peak-valley price ratio is included, which is expressed as Eq. (55). Additionally, the cost limit represents the minimum price that must be charged for electricity during valley period, as in Eq. (56). Finally, there is no load curtailment at PBDR, which means that load consumption before and after applying DR is not changed, as in Eq. (57).

$$\sum_t TLR_t^{DR} \leq DR^{lim} \quad , \forall t \in Pp \quad (51)$$

$$0 \leq inc_p \leq inc_p^{lim} \quad (52)$$

$$\rho_p - \rho_f \geq 0 \quad (53)$$

$$\rho_f - \rho_v \geq 0 \quad (54)$$

$$2 \leq \frac{\rho_p}{\rho_v} \leq 5 \quad (55)$$

$$\rho_v - \rho_v^{lim} \geq 0 \quad (56)$$

$$\sum_{i,t} d_{i,t}^{Before} \leq \sum_{i,t} d_{i,t}^{After} \quad , \forall i \in I, \forall t \in T \quad (57)$$

2.4. Technical Performance Indices

To assess variation degree in load curve over time, load factor has been defined by Eq. (58).

$$load\_factor\% = 100 * \frac{\sum_{t=1}^T d_t}{T * d_t^{max}} \quad , \forall t \in T \quad (58)$$

Other significant factors calculate various percentages between peak and valley. These factors are established using Eq. (59) and Eq. (60).

$$peak\ to\ valley\ distance = 100 * \frac{d_t^{max} - d_t^{min}}{d_t^{max}} \quad (59)$$

$$peak - compensate\% = 100 * \frac{d_{o,t}^{max} - d_t^{max}}{d_{o,t}^{max}} \quad , \forall t \in T \quad (60)$$

As loads are reduced or shifted to make total load profile as flat as possible, load shape is an important factor that is calculated as in Eq. (61).

$$load\_shape = \sum_t (d_t - d_t^{mean})^2 \quad , \forall t \in T \quad (61)$$

To show DR impact on voltage, VDI is used as in Eq. (62). Where voltage at bus (i) during time slot t is represented by  $V_{i,t}$ , and nominal voltage value at bus (i) is indicated by  $V_i^0$ .

$$voltage\ deviation\ index = \frac{\sum_{t=1}^{24} \sum_{i=1}^{33} (V_i^0 - V_{i,t})^2}{T} \quad , \forall t \in T, \forall i \in I \quad (62)$$

2.5. Solution Procedures

2.5.1. Determine Net Load Curve

The net load profile can be estimated by subtracting wind energy output from actual load demand at each time interval. This calculation considers wind energy effect on distribution network and provides a more accurate representation of system's energy demand and supply. The resulting net load profile can then be used to optimize demand response programs and improve efficiency of distribution system [24].

2.5.2. Peak-Valley Time Division

Peak-valley time division refers to process of dividing 24 hours into distinct time intervals that correspond to peak, valley, and flat load periods. Various methods can be used for peak-valley time division, half ladder membership function [25] is utilized here. This method is utilized to classify load curves into distinct periods based on net load curve. Difference between total load demand and wind output yields net load curve. Using half-ladder membership function method, the net load curve is subdivided into three different intervals: peak, valley, and flat periods, derived from the threshold values of maximum and minimum demand. This method provides a simple and effective way to classify load curves into distinct periods, which is essential for implementation of the proposed WCR-DRP.

2.5.3. Apply the Load Economic Model

After obtaining time periods, economic model of each scenario, which includes PBDRP, IBDRP and the proposed DRP, is applied to load curve.

2.5.4. Solving the MOO Problem



There exist several techniques that can be utilized to solve optimization problems involving multiple objective functions, methods such as evolutionary algorithms, weighted sum method, and Pareto optimality are utilized. This paper utilizes Pareto optimality method for solving the proposed optimization problem. Specifically, Pareto optimal front is determined using  $\epsilon$ -constraint method [26], which involves minimizing one objective function by converting remaining objectives into constraints and imposing an upper limit on them. Pareto front is obtained by gradually decreasing this limit until optimal set of solutions is obtained.

2.5.5. Choosing the Best Solution

A fuzzy satisfying approach is utilized to find the best solution from obtained solutions [27]. This technique evaluates extent to which each solution satisfies multiple objectives and selects the solution that achieves the highest degree of objective satisfaction. An explanation of Pareto optimality is provided in [28,29] and the fuzzy satisfying approaches are explained in [30,31].

3. Simulation Results

3.1. Test System Description

To evaluate suggested approach validity, it was tested using enhanced IEEE 33-bus distribution system [32] with wind generation integrated at buses 18, 22, 25, and 33, as illustrated in Fig.2, with some modifications on wind generation units: it is established that wind power cost is negligible and therefore not taken into consideration in this analysis, while wind power output is not taken as a fixed output but as a variable with time, and the assumed hourly wind output power is presented in Table 1.

By considering mesh configuration, the system was modeled with more accuracy, allowing for interactions among various elements of the system to be captured, and thermal unit cost equation is  $0.003P^2 + 12P + 240$  (\$/h) where  $P$  represents unit output power.

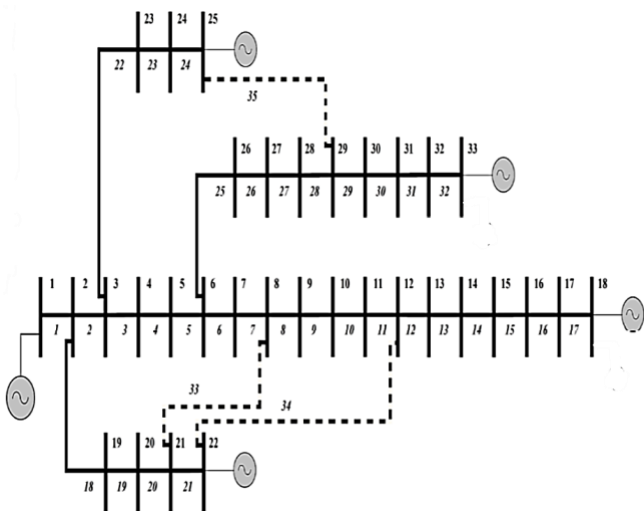


Fig. 2. Enhanced IEEE 33 Bus Distribution Test System

In implementing the proposed approach, the initial flat rate electricity price was set at 150 (\$/MWh), with electricity price limits in valley period at 20% of flat value, respectively. The price of wind curtailment was set at 50 (\$/MWh), and the maximum incentive limit was set at 10 times the flat price. The allowed load for DRP was set at 10% of total load each time. Table 2 provides elasticity coefficient matrix.

Table 1. Day-ahead hourly wind data

Time (hour)	Available wind power (MW)	Percentage of available wind
1	0.547609	0.684511335
2	0.515298	0.64412269
3	0.490455	0.613069156
4	0.479787	0.599733283
5	0.471099	0.588874071
6	0.478415	0.59801867
7	0.501429	0.626786054
8	0.521395	0.651743189
9	0.564831	0.706039246
10	0.629606	0.787007049
11	0.671214	0.839016956
12	0.682187	0.852733854
13	0.696514	0.870642027
14	0.667403	0.834254144
15	0.653229	0.816536483
16	0.655515	0.81939417
17	0.699257	0.874071252
18	0.8	1
19	0.786893	0.983615927
20	0.749095	0.936368832
21	0.710078	0.887597638
22	0.647438	0.809297009
23	0.596685	0.745856354
24	0.586778	0.733473

Table 2. Elasticity coefficient matrix [33]

	Peak	Flat	Valley
Peak	-0.1	0.016	0.012
Flat	0.016	-0.1	0.01
Valley	0.012	0.01	-0.1

Table 3. Result of peak-valley division

Period	Corresponding time
Peak	14,15,16,20,21,22,23,24

Flat	1,9,10,11,12,13,17,18,19
Valley	2,3,4,5,6,7,8

In accordance with net load data, which is given in Fig. 3, load curve is subdivided into three intervals: valley, flat, and peak, and they were arranged as in Table 3. The established model is a MINLP model implemented in GAMS environment [34] and solved using NEOS Server [35] with DICOPT solver [36].

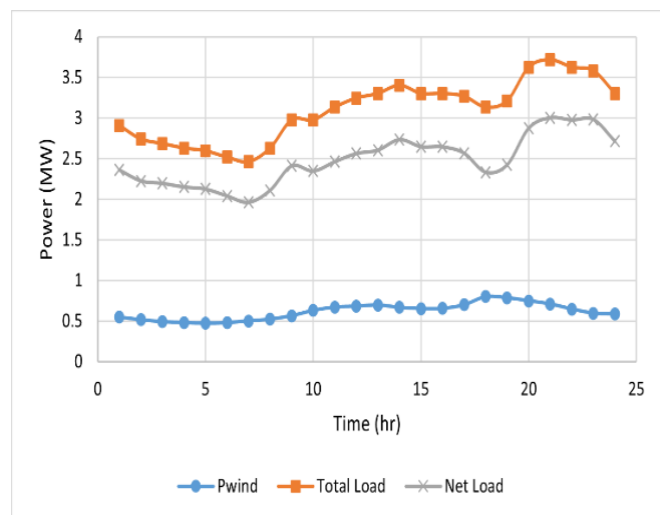


Fig. 3. Hourly load, wind power, and net load

3.2. Optimization Results

The outcomes numerical analyses from both economic and technical perspectives are discussed in this section. To evaluate the proposed approach, several scenarios were considered, as described in Table 4. These scenarios were applied to test system for analysis. The optimization problem was solved, and the optimal solutions based on Pareto optimality were obtained using  $\epsilon$ -constraint method. The best solution for each scenario was then chosen using the fuzzy-satisfying approach. Several indices were determined to evaluate results and provide a comprehensive evaluation of the suggested model, considering needs and perspectives of various stakeholders in distribution system.

Table 4. Description of different scenarios

Scenario1	Base case with no DR program applied. All customers are assumed to be enrolled in flat charge payment plan.
Scenario2	TOU- PBDR is applied
Scenario3	Direct Load Control (DLC) IBDR is applied.
Scenario4	The proposed DRP is applied

3.2.1. Scenario 1

The initial case is scenario 1, where no demand response program (DRP) is implemented, and the customer is charged at a fixed rate of 150 (\$/MWh) for electricity consumption. Using multi-objective function and constraints outlined in Eq. (25) to Eq. (50), optimization results indicate that the minimum operating cost is achieved at wind curtailment minimum value. In this scenario, operating cost amounts to 6534.9 (\$) and associated wind-curtailed power is 685 (kW), and other technical and economic outcomes are outlined in Table 12. and Table 13. respectively. Absence of DR, limits ability to adjust electricity consumption pattern to better match the available wind power generation, leading to increased wind curtailment and higher operating costs.

3.2.2. Scenario 2

In this scenario, an IBDR is applied, in which incentive payments are given to customers to adjust their usage to lower consumption during peak demand periods. Optimization analysis utilized multi-objective function and constraints outlined in Eq. (25) to Eq. (52). Electricity price was set at 150 (\$/MWh), and the maximum incentive limit was set to be 10 times the flat price. Additionally, the allowed load for DRP was set at 10% of total load each time. Using these parameters, Pareto front and the optimal solution are presented in Fig. 4 and Table 5.

Solution #7 is chosen as the best one, with a total operating cost of 6596.4 (\$) and 379.4 (kW) curtailed power. The associated incentive value at peak period is 72.43 (\$/MWh). As illustrated in Fig.5, a load reduction occurred during peak periods, and other technical and economic outcomes are shown in Table 12. and Table 13. respectively.

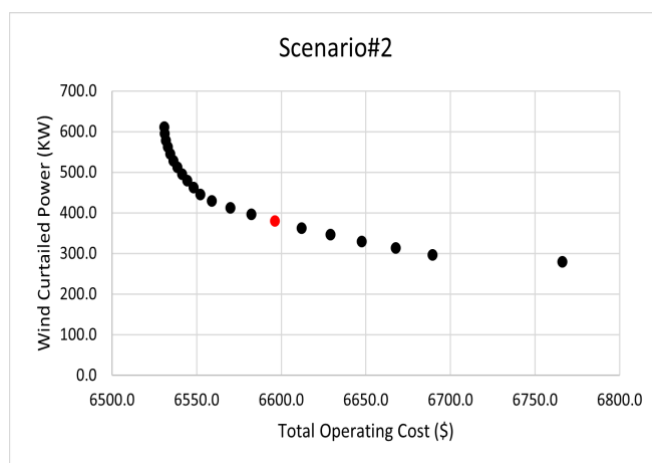


Fig. 4. Pareto front of Scenario 2

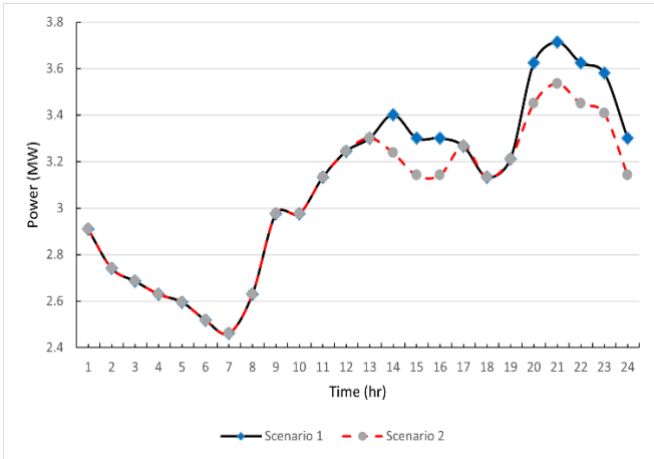


Fig. 5. Load curves of scenarios 1 and 2

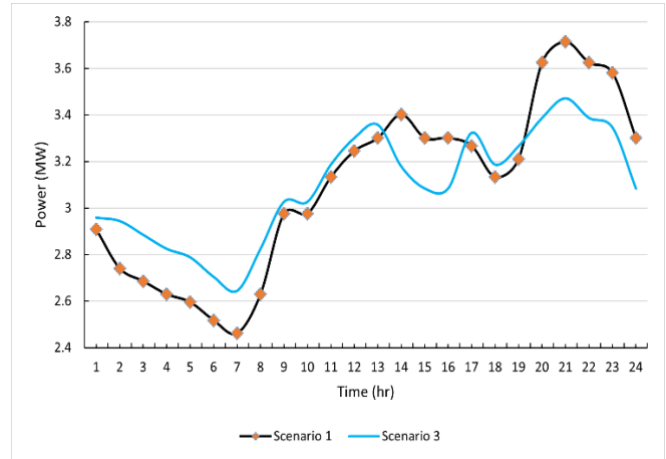


Fig. 6. Load curves of scenarios 1 and 3

Table 5. Pareto optimal solutions for scenario 2

Solution number	$OF_1$	$OF_2$	$\mu_1$	$\mu_2$	$\mu^n$
1	6766.1	280.0	0.000	1.000	0.000
2	6689.3	296.6	0.327	0.950	0.327
3	6667.7	313.1	0.418	0.900	0.418
4	6647.6	329.7	0.504	0.850	0.504
5	6629.0	346.3	0.583	0.800	0.583
6	6612.0	362.9	0.656	0.750	0.656
7	6596.4	379.4	0.722	0.700	0.700
8	6582.4	396.0	0.781	0.650	0.650
9	6569.9	412.6	0.834	0.600	0.600
10	6559.0	429.2	0.881	0.550	0.550
11	6552.1	445.7	0.910	0.500	0.500
12	6548.1	462.3	0.927	0.450	0.450
13	6544.6	478.9	0.942	0.400	0.400
14	6541.4	495.5	0.956	0.350	0.350
15	6538.7	512.1	0.967	0.300	0.300
16	6536.4	528.6	0.977	0.250	0.250
17	6534.5	545.2	0.985	0.200	0.200
18	6533.0	561.8	0.992	0.150	0.150
19	6531.9	578.4	0.996	0.100	0.100
20	6531.2	594.9	0.999	0.050	0.050
21	6531.0	611.5	1.000	0.000	0.000

3.2.3. Scenario 3

In this case, a PBDR program based on TOU pricing is applied. Optimization analysis was conducted using multi-objective function and constraints outlined in Eq. (25) to Eq. (50) and Eq. (53) to Eq. (57). Additionally, electricity price limit for valley periods was set to be 20% of the flat value, respectively. In this scenario, the minimum value of operating cost occurs at the minimum value of wind curtailed power, with a total operating cost of 6498.62 (\$) and 107.5815 (kW) of curtailed power. The associated electricity prices at peak, flat, and valley periods were 232.602, 127.375, and 46.5204 (\$/MWh) respectively. As illustrated in Fig. 6, a load shifting has occurred, customers shifted their load from peak to valley and flat periods, and other technical and economic outcomes are outlined in Table 12. and Table 13. respectively.

3.2.4. Scenario 4

In this case, the proposed DRP, Wind Curtailment Reduction DRP (WCR-DRP). The generator considered in this study has a ramp-up limit of 0.2 MW, a ramp-down limit of 0.2 MW, and a minimum output power of 0 MW. After applying optimal power flow, the determined critical times are 7, 8, 18, 19 as critical up time, and 24 as critical down time.

Then, optimization analysis was conducted using multi-objective function and constraints outlined in Eq. (1) to Eq. (50) and Eq. (53) to Eq. (57).

The best solution is found for both operating cost and total wind curtailed power, with a total operating cost of 6491.89 (\$) zero (kW) curtailed power. The associated electricity prices at peak, flat, and valley periods are 234.213, 128.99, and 46.8426 (\$/MWh) respectively, the associated electricity prices during critical times at peak, flat, and valley periods are 304.094, 78.4006, and 60.8188 (\$/MWh) respectively. As can be seen in Fig. 7 and Fig. 8, a load shift has occurred as in scenario 3, but more consumption has been shifted from hour 23 at peak period to hours 18, 19 at flat period due to different prices at these times, which results a zero-wind curtailed power. Finally, other technical and economical outcomes are outlined in Table 12. and Table 13. respectively. Furthermore, binary variables and electricity prices associated with the best solution of the suggested DR program are given in Tables 6, 7, and Table 8. respectively.

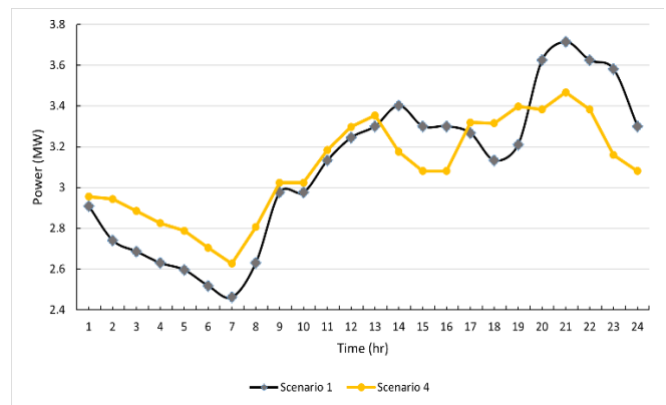


Fig. 7. Load curves of scenarios 1 and 4

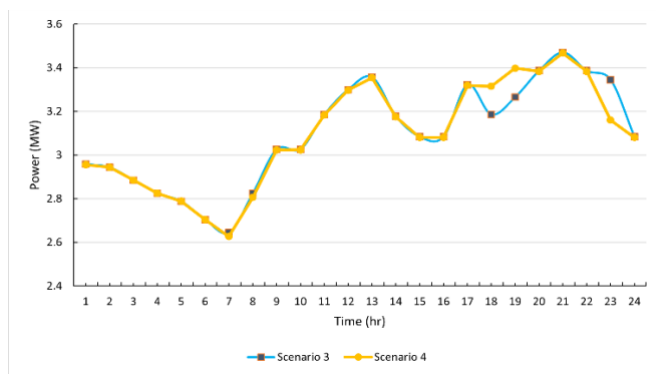


Fig. 8. Load curves of scenarios 3 and 4

Table 6. Binary variables of suggested model

Time (hour)	$\alpha_{v, tcr}$	$\alpha_{f, tcr}$	$\beta_{p, tcr}$	$\beta_{f, tcr}$
1	0	0	0	0
2	0	0	0	0
3	0	0	0	0
4	0	0	0	0
5	0	0	0	0
6	0	0	0	0
7	0	0	0	0
8	0	0	0	0
9	0	0	0	0
10	0	0	0	0
11	0	0	0	0
12	0	0	0	0
13	0	0	0	0
14	0	0	0	0
15	0	0	0	0
16	0	0	0	0
17	0	0	0	0
18	0	0	0	1
19	0	0	0	1
20	0	0	0	0
21	0	0	0	0
22	0	0	0	0
23	0	0	0	0
24	0	0	0	0
Time (hour)	$\beta_{v, tcr}$	$\gamma_{p, tcr}$	$\gamma_{f, tcr}$	$\gamma_{v, tcr}$
1	0	0	0	0
2	0	0	0	0
3	0	0	0	0
4	0	0	0	0
5	0	0	0	0
6	0	0	0	0
7	1	0	0	0
8	1	0	0	0
9	0	0	0	0
10	0	0	0	0

11	0	0	0	0
12	0	0	0	0
13	0	0	0	0
14	0	0	0	0
15	0	0	0	0
16	0	0	0	0
17	0	0	0	0
18	0	0	0	0
19	0	0	0	0
20	0	0	0	0
21	0	0	0	0
22	0	0	0	0
23	0	0	0	0
24	0	1	0	0

Table 7. Binary variables of suggested model

Time (hour)	$Xv_t$	$Xf_t$	$Xp_{up_{tcr}}$	$Xp_{dw_{tcr}}$
1	0	0	0	0
2	0	0	0	0
3	0	0	0	0
4	0	0	0	0
5	0	0	0	0
6	0	0	0	0
7	1	0	0	0
8	1	0	0	0
9	0	0	0	0
10	0	0	0	0
11	0	0	0	0
12	0	0	0	0
13	0	0	0	0
14	0	0	0	0
15	0	0	0	0
16	0	0	0	0
17	0	0	0	0
18	0	1	0	0
19	0	1	0	0
20	0	0	0	0
21	0	0	0	0
22	0	0	0	0
23	0	0	0	0
24	0	0	0	1

Table 8. Electricity prices during each time of day

Time (hour)	Electricity price (\$/MWh)
1	128.99
2	46.8426
3	46.8426
4	46.8426
5	46.8426
6	46.8426
7	60.8188
8	60.8188

9	128.99
10	128.99
11	128.99
12	128.99
13	128.99
14	234.213
15	234.213
16	234.213
17	78.4006
18	78.4006
19	128.99
20	234.213
21	234.213
22	234.213
23	304.094
24	234.213

3.3. Results Analysis

This section covers findings obtained from various scenarios.

3.3.1. Pareto Optimal Solution Comparison

Results obtained from Pareto optimal front at each scenario presented above are used to determine ranges of variation for the objective functions in different scenarios, as outlined in Table 9. and depicted in Fig. 9, Fig. 10, and Fig. 11. The investigation of results shows that solutions obtained by the suggested model dominate those of other cases. This means that the minimum operating cost and the minimum wind curtailed power have been obtained. It is noteworthy that the minimum curtailed wind power that can be obtained from the suggested model is zero (kW). This means that the suggested model can effectively eliminate curtailed energy, which cannot be achieved by other scenarios.

**Table 9.** Comparison of objective results for each scenario

Scenario	Max $OF_1$ (\$)	Min $OF_1$ (\$)	Max $OF_2$ (kW)	Min $OF_2$ (kW)
1	6534.9	6534.9	685.0	685.0
2	6766.1	6531.0	611.5	280.0
3	6498.6	6498.6	107.6	107.6
4	6491.89	6491.89	-	-

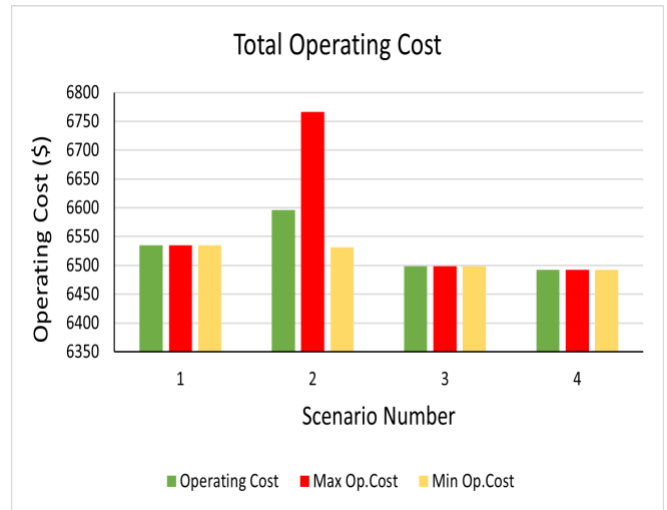


**Fig. 9.** Min, Max, and the chosen value of total operating cost of different scenarios

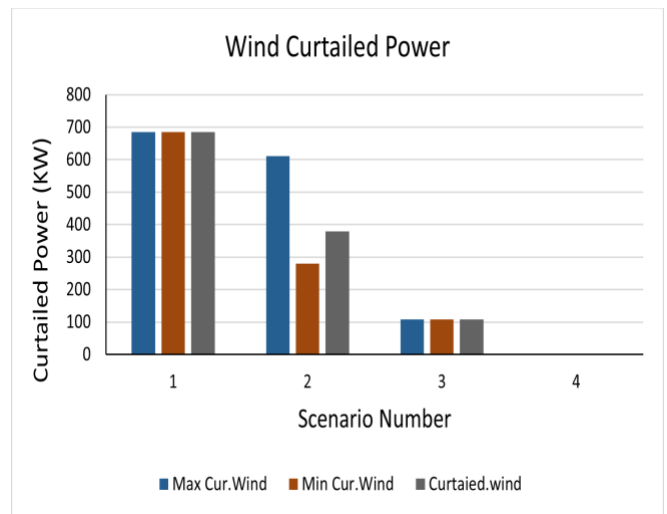


**Fig. 10.** Min, Max, and chosen value of wind-curtailed power of different scenarios

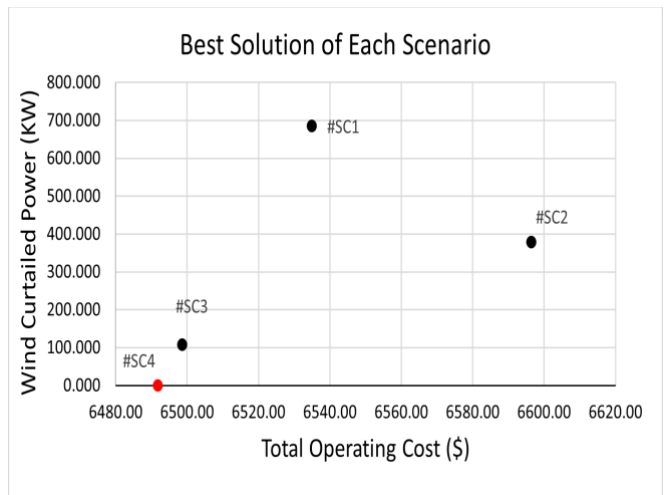


**Fig. 11.** Best solution of each scenario

3.3.2. Wind Power Output

Hourly output of wind power for each case is presented in Table 10. and Fig. 12

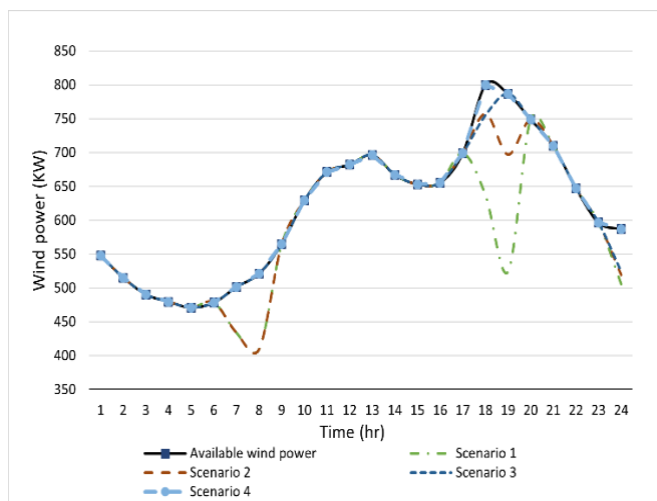


Fig. 12. Wind output power of different scenarios

Table 10. Output wind power at each scenario

Time (hour)	Available wind power	Scenario 1	Scenario 2	Scenario 3
1	0.548	0.548	0.548	0.548
2	0.515	0.515	0.515	0.515
3	0.490	0.490	0.490	0.490
4	0.480	0.480	0.480	0.480
5	0.471	0.471	0.471	0.471
6	0.478	0.478	0.478	0.478
7	0.501	0.434	0.434	0.501
8	0.521	0.410	0.410	0.521
9	0.565	0.565	0.565	0.565
10	0.630	0.630	0.630	0.630
11	0.671	0.671	0.671	0.671
12	0.682	0.682	0.682	0.682
13	0.697	0.697	0.697	0.697
14	0.667	0.667	0.667	0.667
15	0.653	0.653	0.653	0.653
16	0.656	0.656	0.656	0.656
17	0.699	0.699	0.699	0.699
18	0.800	0.637	0.757	0.755
19	0.787	0.524	0.697	0.787
20	0.749	0.749	0.749	0.749
21	0.710	0.710	0.710	0.710
22	0.647	0.647	0.647	0.647
23	0.597	0.597	0.597	0.597
24	0.587	0.506	0.519	0.524
Time (hour)	Available wind power	Scenario4		
1	0.548	0.548		
2	0.515	0.515		
3	0.490	0.490		
4	0.480	0.480		
5	0.471	0.471		
6	0.478	0.478		

7	0.501	0.501
8	0.521	0.521
9	0.565	0.565
10	0.630	0.630
11	0.671	0.671
12	0.682	0.682
13	0.697	0.697
14	0.667	0.667
15	0.653	0.653
16	0.656	0.656
17	0.699	0.699
18	0.800	0.800
19	0.787	0.787
20	0.749	0.749
21	0.710	0.710
22	0.647	0.647
23	0.597	0.597
24	0.587	0.587

Results of the investigation into critical times and wind output power have provided evidence to support the concept that wind curtailment occurrences are related to ramp-up/down limits of the generator. In each scenario considered in this study, wind-curtailed power occurred at critical times.

Thus, by taking into account ramp-up/down limits of generator, it is possible to improve the accuracy of the DR programs and optimize the operation of power system to reduce wind curtailment.

### 3.3.3. Proposed Model Analysis

In this section an analysis of the suggested method is investigated. As indicated in the results,

$$Xf_t = \begin{cases} 1 & \text{at } t = 18,19 \\ ,0 & \text{otherwise} \end{cases}$$

$$Xv_t = \begin{cases} 1 & \text{at } t = 7,8 \\ ,0 & \text{otherwise} \end{cases}$$

$$Xp_{up_{tcr}} = \{0 \text{ at all times}\}$$

$$Xp_{dw_{tcr}} = \begin{cases} 1 & \text{at } t = 24 \\ ,0 & \text{otherwise} \end{cases}$$

Which mean that the ramping limits could be breached at certain critical times during the valley period ( $t = 7,8$ ), flat period ( $t = 18,19$ ), and peak period ( $t = 24$ ), which increase the likelihood of wind curtailment events. The wind output power subsection above identifies wind curtailments at various scenarios, as presented in Table 11.

Table 11. Wind curtailment times

Scenario	Wind curtailment times (hr)
1	$t = 7, 8, 18, 19, 24$
2	$t = 7, 8, 18, 19, 24$
3	$t = 18, 24$

4	-
---	---

In Scenario 2, where the incentive-based demand response program (IBDRP) is applied, there is no notable change in wind curtailment hours. This is because IBDRP only focuses on load reduction during peak hours, which is not effective in mitigating wind curtailment.

Scenario 3 exhibits a reduction in wind curtailment power due to the application of price-based demand response program (DRP), which shifts the load from peak hours to valley and flat hours. This reduces wind curtailment at some times during valley and flat periods by increasing the load. However, wind curtailment cannot be eliminated at  $t = 18$  due to high wind power and at  $t = 24$  due to reduced load at peak period, which does not help in reducing curtailment.

However, in scenario 4, the proposed DR model adjusts electricity prices during critical times of valley and flat periods ( $t = 7,8,18,19$ ) and at  $t = 23$  during peak period when the ramping limit is met due to ramping down. This effectively eliminates wind curtailment at all times.

Overall, this section highlights the innovative approach used in this study by adjusting the demand response program during critical technical times of generators, which helps to reduce wind curtailments and promote the integration of more renewable energy.

3.3.4. Technical Comparison

In this section, various technical parameters that are critical to the distribution network's optimal operation are outlined.

These parameters include minimum bus voltage, peak and valley loads, VDI, active and reactive power losses, load factor, load shape, peak-valley distance, and peak-compensate.

At each scenario's best solution, technical aspects of load profile of test system are outlined in Table 12.

The results shown in Table 12. demonstrate that implementing demand response programs (DRPs) leads to improvements in technical parameter values in contrast to the base case with no DRP. The suggested model (Scenario 4) outperforms single PBDR or IBDR approaches, achieving the best load factor and peak-compensate factors of 89.4% and 6.7%, respectively. Scenario 3 and Scenario 4 achieved the best load shape of 1.3 and peak-valley distances of around 24%.

Additionally, scenario 2 resulted in the least system losses and Voltage Deviation Index (VDI) as load reduction occurred in this scenario. Results establish the performance of the suggested model in improving technical performance of the power system while also reducing energy waste and costs.

**Table 12.** Technical comparison of scenarios

Scenario	Min V (P.U)	Load peak (MW)	Load valley (MW)	P-loss (MW)	Peak-valley Distance (%)
1	0.959	3.715	2.462	1.528	33.7
2	0.960	3.536	2.462	1.470	30.4
3	0.961	3.471	2.644	1.493	23.8
4	0.961	3.467	2.626	1.488	24.2
Scenario	Q-loss	Load Shape	VDI	Load factor (%)	Peak-compensate (%)
1	1.068	3.3	0.018	83	0
2	1.026	2.4	0.017	85.93	4.8
3	1.043	1.3	0.017	89	6.5
4	1.040	1.3	0.017	89.42	6.7

3.3.5. Economical Comparison

In this section, economic characteristics of the load profile for each scenario's best solution are presented, including total operating cost (decomposed into generation cost, wind curtailment cost, and DR cost) and the cost of customer bill which are reported in Table 13.

**Table 13.** Economical comparison of scenarios

Scenario	Generation Cost (\$)	Wind Curtailment Cost (\$)	DR Cost (\$)
1	6500.61	34.30	-
2	6480.06	18.97	97.39
3	6493.24	5.38	-
4	6491.89	-	-
Scenario	Total Operating Cost (\$)	Customer Bill (\$)	Bill Reduction (%)
1	6534.91	11139.8	-
2	6596.43	10840.6	2.68
3	6498.62	10611.4	4.74
4	6491.89	10644.2	4.45

The suggested model has a minimum total operating cost of 6491.89 (\$), which is the best scenario from a utility point of view. This result indicates that the suggested DR program is able to minimize operating costs of system. Whereas, scenario 2, in which IDPD is implemented, has a maximum operating cost of 6596.43 (\$) and a DR cost of 97.39 (\$),



making it the least desirable scenario in terms of total operating cost.

From the viewpoint of customer, the suggested model leads to a 4.45% bill reduction, which is almost equal to bill reduction obtained from Scenario 3. This result indicates that the suggested DR program can provide significant financial benefits to customers while also improving technical performance of power system.

#### 4. Conclusion

This paper outlines a strategy for optimal operation of distribution systems, taking into account impact of DR programs and wind curtailment energy. The suggested DR program adjusts electricity prices at critical times at which wind curtailments may occur due to ramp-up/down limits or minimum generator output limit, to encourage load shifting and eliminate curtailed wind power. The approach is presented as a multi-objective optimal power flow (OPF) problem with objectives of minimizing total utility operating cost and its corresponding curtailed wind power.

The simulation experiments conducted on the enhanced IEEE 33-bus system demonstrate the superiority of Scenario #4, which utilizes the proposed demand response program (DRP), in providing the most desirable technical characteristics compared to other scenarios. Based on the results, the proposed model achieved a curtailed wind power output of zero while simultaneously achieving a high load factor of 89.4% compared with 83% of base case, which indicate the effectiveness of the proposed DRP in reducing wind curtailment and improving the technical performance of the power system.

Moreover, the suggested model exhibited superior economic characteristics by significantly reducing the daily operating cost to \$6,491.89 compared to \$6,534.90 in the base case. The proposed model also resulted in a reduction of customer bills by 4.5% relative to the base case, indicating its potential benefits to the utility and customers. These significant values for power system, utility, and customers illustrate the effectiveness of the proposed DRP in improving the overall performance of distribution systems.

Overall, findings suggest that the suggested approach is a powerful approach for enhancing performance of distribution networks while considering impacts of DR programs and wind curtailment power, which be used to inform policy decisions and improve the reliability and efficiency of future intelligent distribution networks.

Future research may integrate wind and load uncertainties into the model and comparing it with an Energy Storage System (ESS) approach.

#### References

- [1] F. Ayadi, I. Colak, I. Garip, and H. I. Bulbul, "Impacts of renewable energy resources in smart grid," in 2020 8th International Conference on Smart Grid (icSmartGrid), 2020.
- [2] International Energy Agency, *Renewables 2022: Analysis and forecast to 2027*. OECD, 2022.
- [3] "Forecasting of short-term and long-term wind speed of Ras Gharib using time series analysis," *Int. J. Renew. Energy Res.*, no. V13i1, 2023.
- [4] L. Bird et al., "Wind and solar energy curtailment: A review of international experience," *Renew. Sustain. Energy Rev.*, vol. 65, pp. 577–586, 2016.
- [5] O. Agbonaye, P. Keatley, Y. Huang, F. O. Odiase, and N. Hewitt, "Value of demand flexibility for managing wind energy constraint and curtailment," *Renew. Energy*, vol. 190, pp. 487–500, 2022.
- [6] U. Cetinkaya, R. Bayindir, and S. Ayik, "Ancillary services using battery energy systems and demand response," in 2021 9th International Conference on Smart Grid (icSmartGrid), 2021.
- [7] N. G. Paterakis, O. Erdinç, and J. P. S. Catalão, "An overview of Demand Response: Key-elements and international experience," *Renew. Sustain. Energy Rev.*, vol. 69, pp. 871–891, 2017.
- [8] P. Siano, "Demand response and smart grids—A survey," *Renew. Sustain. Energy Rev.*, vol. 30, pp. 461–478, 2014.
- [9] I. I. R. Gomes, R. Melicio, and V. M. F. Mendes, "Aggregation of wind, photovoltaic and thermal power with demand response," in 2019 8th International Conference on Renewable Energy Research and Applications (ICRERA), 2019.
- [10] U. Cetinkaya and R. Bayindir, "Impact of increasing renewable energy sources on power system stability and determine optimum demand response capacity for frequency control," in 2022 10th International Conference on Smart Grid (icSmartGrid), 2022.
- [11] E. E. El-Araby and N. Yorino, "A demand side response scheme for enhancing power system security in the presence of wind power," *Int. J. Electr. Power Energy Syst.*, vol. 146, no. 108714, p. 108714, 2023.
- [12] M. Rahmani-Andebili, "Modeling nonlinear incentive-based and price-based demand response programs and implementing on real power markets," *Electric Power Syst. Res.*, vol. 132, pp. 115–124, 2016.
- [13] D. S. Kirschen, G. Strbac, P. Cumperayot, and D. de Paiva Mendes, "Factoring the elasticity of demand in electricity prices," *IEEE Trans. Power Syst.*, vol. 15, no. 2, pp. 612–617, 2000.
- [14] A. Asadinejad and K. Tomsovic, "Optimal use of incentive and price-based demand response to reduce costs and price volatility," *Electric Power Syst. Res.*, vol. 144, pp. 215–223, 2017.
- [15] M. Nikzad and B. Mozafari, "Reliability assessment of incentive- and priced-based demand response programs in



- restructured power systems,” *Int. J. Electr. Power Energy Syst.*, vol. 56, pp. 83–96, 2014.
- [16] H. A. Aalami, M. P. Moghaddam, and G. R. Yousefi, “Modeling and prioritizing demand response programs in power markets,” *Electric Power Syst. Res.*, vol. 80, no. 4, pp. 426–435, 2010.
- [17] Q. Xu, Y. Ding, and A. Zheng, “An optimal dispatch model of wind-integrated power system considering demand response and reliability,” *Sustainability*, vol. 9, no. 5, p. 758, 2017.
- [18] V. C. Pandey, N. Gupta, K. R. Niazi, A. Swarnkar, and R. A. Thokar, “Modeling and assessment of incentive-based demand response using price elasticity model in distribution systems,” *Electric Power Syst. Res.*, vol. 206, no. 107836, p. 107836, 2022.
- [19] J. Jiang, Y. Kou, Z. Bie, and G. Li, “Optimal real-time pricing of electricity based on demand response,” *Energy Procedia*, vol. 159, pp. 304–308, 2019.
- [20] H. Yang, L. Wang, and Y. Ma, “Optimal time of use electricity pricing model and its application to electrical distribution system,” *IEEE Access*, vol. 7, pp. 123558–123568, 2019.
- [21] X. Zhou, J. Shi, and G. Kang, “Optimal demand response aiming at enhancing the economy of high wind power penetration system,” *J. Eng. (Stevenage)*, vol. 2017, no. 13, pp. 1959–1962, 2017.
- [22] H. Falsafi, A. Zakariazadeh, and S. Jadid, “The role of demand response in single and multi-objective wind-thermal generation scheduling: A stochastic programming,” *Energy (Oxf.)*, vol. 64, pp. 853–867, 2014.
- [23] H. Xu, Y. Chang, Y. Zhao, and F. Wang, “A new multi-timescale optimal scheduling model considering wind power uncertainty and demand response,” *Int. J. Electr. Power Energy Syst.*, vol. 147, no. 108832, p. 108832, 2023.
- [24] H. Bitaraf and S. Rahman, “Reducing curtailed wind energy through energy storage and demand response,” *IEEE Trans. Sustain. Energy*, vol. 9, no. 1, pp. 228–236, 2018.
- [25] N. Li, X. Wang, Z. Zhu, and Y. Wang, “The reliability evaluation research of distribution system considering demand response,” *Energy Rep.*, vol. 6, pp. 153–158, 2020.
- [26] F. Ugranlı, “Analysis of renewable generation’s integration using multi-objective fashion for multistage distribution network expansion planning,” *Int. J. Electr. Power Energy Syst.*, vol. 106, pp. 301–310, 2019.
- [27] M. Basu, “An interactive fuzzy satisfying method based on evolutionary programming technique for multiobjective short-term hydrothermal scheduling,” *Electric Power Syst. Res.*, vol. 69, no. 2–3, pp. 277–285, 2004.
- [28] A. Soroudi, M. Ehsan, R. Caire, and N. Hadjsaid, “Hybrid immune-genetic algorithm method for benefit maximisation of distribution network operators and distributed generation owners in a deregulated environment,” *IET Gener. Transm. Distrib.*, vol. 5, no. 9, pp. 961–972, 2011.
- [29] A. Soroudi, *Power system optimization modeling in GAMS*, 1st ed. Basel, Switzerland: Springer International Publishing, 2017.
- [30] I. J. Ramirez-Rosado and J. A. Dominguez-Navarro, “Possibilistic model based on fuzzy sets for the multi objective optimal planning of electric power distribution networks,” *IEEE Trans. Power Syst.*, vol. 19, no. 4, pp. 1801–1810, 2004.
- [31] M.-R. Haghifam, H. Falaghi, and O. P. Malik, “Risk-based distributed generation placement,” *IET Gener. Transm. Distrib.*, vol. 2, no. 2, p. 252, 2008.
- [32] S. H. Dolatabadi, M. Ghorbanian, P. Siano, and N. D. Hatziargyriou, “An Enhanced IEEE 33 Bus Benchmark Test System for Distribution System Studies,” *IEEE Trans. Power Syst.*, vol. 36, no. 3, pp. 2565–2572, 2021.
- [33] J. J. Chen, B. X. Qi, K. Peng, Y. Li, and Y. L. Zhao, “Conditional value-at-credibility for random fuzzy wind power in demand response integrated multi-period economic emission dispatch,” *Appl. Energy*, vol. 261, no. 114337, p. 114337, 2020.
- [34] M. R. Bussieck and A. Meeraus, *General Algebraic Modeling System (GAMS)*, in *Applied Optimization*. Boston, MA: Springer US, 2004.
- [35] J. Czyzyk, M. P. Mesnier, and J. J. More, “The NEOS Server,” *IEEE Comput. Sci. Eng.*, vol. 5, no. 3, pp. 68–75, 1998.
- [36] G. R. Kocis and I. E. Grossmann, “Computational experience with dicopt solving MINLP problems in process systems engineering,” *Comput. Chem. Eng.*, vol. 13, no. 3, pp. 307–315, 1989.